# Surface Phase Transition of Associating Fluids on Functionalized Surfaces

Sandip Khan and Jayant K. Singh*

Department of Chemical Engineering, Indian Institute of Technology Kanpur, Kanpur 208016, India

ABSTRACT: Surface phase transitions are studied for Lennard-Jones (LJ) based dimer forming associating fluids on modified surfaces with active sites for various association strengths using grand-canonical transition matrix Monte Carlo. We examine adsorption isotherm, density, energy, and monomer profiles to differentiate layering, quasi-2D vapor—liquid and prewetting transitions. Prewetting transition is found for association strengths: $\varepsilon_{af} = 8$ and 10, whereas, for weaker associating fluids, $\varepsilon_{af} = 4$ and 6, we observe quasi-2D vapor—liquid transition. The growth of thick films in the case of quasi-2D vapor liquid transitions is found to suppress with decrease in temperature and eventually splits in layering transitions. For systems exhibiting prewetting transition, wetting temperature and prewetting critical temperature increase with increasing association strength. In addition, we examine boundary tension of quasi-2D and prewetting transitions using finite size scaling formalism of Binder. Our results indicate that the quasi-2D boundary tension is lower than that of the prewetting transition. Surface sites are found to reduce the boundary tension; however, the effect of active sites diminishes with stronger fluid—fluid associating strength.
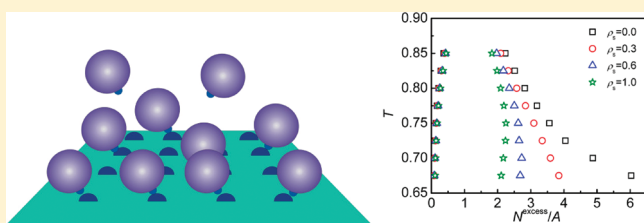
1. INTRODUCTION

Fluid behavior near the surface, in particular wetting transition, is actively being studied due to its potential application in microcontact printing,[1] coating,[2] molecular electronics or optical devices,[3] biochemical sensor,[4] microfluidics devices,[5] etc. Wetting transition, a surface phase transition, from partial wetting to complete wetting is usually found to be a first-order transition characterized by a discontinuous jump (observed in the thickness of the adsorbed film) from a microscopically thin adsorbed film (coexistence with the droplet) to a macroscopically thick film. Prior to the wetting transition, in the gas phase, i.e., off bulk coexistence, prewetting transition may appear where microscopic thin film coexists with comparatively thicker film along with the gas phase. The prewetting transition stems from a saturation curve at wetting temperature (T_W) and strongly depends on the substrate strength. Prewetting transition can be suppressed easily for many systems as it is observed at a very close to the vapor—liquid coexistence line and associated with many interactions at the solid—fluid interface. Due to this fact, despite the prediction by theoretical methods in 1977[6,7] and subsequently by Monte Carlo simulations in 1989[8] experimental evidence came much later in 1992.[9] Examples can be found from simple systems (helium on Cs[9,10] and Rb,[11] liquid hydrogen on various substrates[12]) to complex systems (acetone on graphite,[13] water on graphite,[14] binary liquid mixture methanol—cyclohexane,[15] liquid pentane on water,[16] binary liquid-crystal systems[17]).

Beside the prewetting transition, one may find other complex surface phase behavior, such as layering transition, capillary condensation, quasi liquid—vapor transition, percolation, and higher order wetting transition, depending on the relative interaction of solid—fluid and state conditions.[18] Control over such phase behavior is still challenging from a technological perspective. In this direction, surface modification can play an important role in inducing/controlling surface phase behavior. Some substrate like metal oxide has inherent attractive sites that can form a network like structure with polar molecules through hydrogen bonding and can influence different phase transitions at the interface. In addition, surface sites inside porous materials like activated carbon, zeolite, activated alumina, etc., can influence the adsorption behavior of polar molecules. Understanding the behavior of such systems requires deep insight at the molecular level. Hence many investigations have been made with associating fluid on modified surfaces.[19−28] It is well understood that a heterogeneous surface or surface sites have significant effect on adsorption behavior[21,22,24] and can lead to different surface phase transitions like interfacial percolation,[20] capillary condensation, layering transition,[23,25] prewetting transition,[26] dewetting transition,[27] etc. Recently, Borowko and co-workers[29] also found crossover behavior of prewetting transition and layering transition in the presence of preadsorbed chain on the surface. However, apart from many well-known surface phase transitions, surface modification may lead to some quasi surface phase transition which is not well understood as seen for simple fluid models. As for example, Sacquin et al.[30] observed, for LJ particles, that introducing a spherical cap at one surface end can induce a partially condensed phase while prewetting transition disappears. Subsequently, in their next work,[31] they found that a

higher chemical potential is required for the prewetting transition at a corrugated surface compare to the plane surface and the prewetting transition can be suppressed by increasing the degree of corrugation. The work of Curtarolo and co-workers[32] indicates that even an impurity or defect on the surface may set different phase transitions. Their grand-canonical Monte Carlo investigation of wetting transition of Ne on a Mg surface suggests that the presence of adatom or hole on the surface can suppress the prewetting transition and can lead to some quasi-transition with depression of the film growth. Similar behavior is also found for square well fluids on a square well based substrate in our earlier work,[33] where distinct the fluid—fluid interaction range for prewetting transition and quasi-2D transition is observed. Further, a different wall—fluid interaction range can interplay between prewetting and layering transition.[34] Similarly, Rull et al.[35] also observed first-order transition for a liquid crystal near the attractive surface between a disordered film and nematic-like film without any hints of prewetting transition. Along with theoretical and simulation study of fluid behavior near modified/functionalized surfaces, extensive studies have been performed experimentally to understand the surface morphology effect on the surface phase transtion.[36−39] A recent review of Taborek[40] summarizes experimental observations of adsorption behavior of quantum fluids on weakly binding alkali metal substrate and discussed surface phase transitions including prewetting and 2D vapor liquid transitions.

While multiple studies on prewetting transition have been conducted, prewetting transition studies of associating and molecular fluids are sparse.[13,14,41,42] Our earlier work[43] on associating fluids on a structureless surface suggests that prewetting transition can be observed for multiple sites associating fluids such as hydrogen fluoride, water, alkanols, and other organic fluids. In this work, we investigate the influence of the surface sites and its density on surface phase transition of one site associating fluids between prewetting transitions and quasi-2D vapor liquid transition. The rest of the paper is organized as follows: section 2 describes the models and simulation methods used in this study. Simulation details are in section 3. Section 4 presents the results and discussion followed by conclusion in section .

2. MODEL AND METHODOLOGY

2.1. Model. In this work, Lennard-Jones potential is used for isotropic van der Waals interactions between fluid molecules. Square-well model is used to represent the off-center orientationally depended associating sites. These sites mimic the strong and short-range directional attraction of real associating fluids. The complete potential model[44] for fluid—fluid interaction is

$$u_{ff}(r_{ij}, \theta_i, \theta_j) = u_{LJ\text{-}tr}(r_{ij}) + u_{af}(r_{ij}, \theta_i, \theta_j)$$

$$u_{af}(r_{ij}, \theta_i, \theta_j) = \begin{cases} -\varepsilon_{af} & \text{if } \sigma < r_{ij} < r_c, \theta_i < \theta_c, \text{ and } \theta_j < \theta_c \\ 0 & \text{Otherwise} \end{cases}$$

(1)

$$u_{LJ\text{-}tr}(r_{ij}) = \begin{cases} 4\varepsilon\left[\left(\dfrac{r_{ij}}{\sigma}\right)^{12} - \left(\dfrac{r_{ij}}{\sigma}\right)^{6}\right] & \text{if } r_{ij} \leq r_{cut} \\ 0 & \text{Otherwise} \end{cases}$$
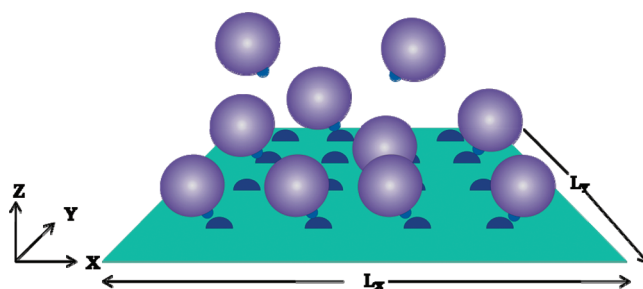

Figure 1. Schematic diagram of associating molecule on surface with associating sites.

where θ_i and θ_j are angles between the center to center vector and the center to site vector of molecules i and j, respectively. ε_{af} is the association well depth and r_c is the range of associating potential. σ and ε are the molecular size and energy parameters of the LJ potential. r_{cut} is the cutoff diameter for the LJ potential. We adopt units such that σ and ε are unity. In this study, θ_c, r_c, and r_{cut} are fixed at 27°, 1.00, and 2.5, respectively.

In this work, a structureless substrate with active sites is used. Sites are distributed uniformly on a rectangular grid on the surface as shown in Figure 1. Substrate—fluid molecular interaction at a distance z is specified by the expression

$$u_{wf} = u_{LJ\text{-}93}(z) + u_{aw}(r_{ij}, \theta_i, \theta_j)$$

$$u_{LJ\text{-}93}(z) = \frac{2\pi}{3}\rho_w\sigma_w^3\varepsilon_w\left[\frac{2}{15}\left(\frac{\sigma_w}{z}\right)^9 - \left(\frac{\sigma_w}{z}\right)^3\right] \quad (2)$$

$$u_{aw}(r_{ij}, \theta_i, \theta_j) = \begin{cases} -\varepsilon_{aw} & \text{if } \sigma < r_{ij} < r_c, \theta_i < \theta_c, \text{ and } \theta_j < \theta_c \\ 0 & \text{Otherwise} \end{cases}$$

where $\rho_w\sigma_w^3$, $\varepsilon_w/\varepsilon$, and σ_w/σ are set to 0.988, 1.2771, and 1.0962, respectively, which corresponds to the argon—solid CO_2 system.[7] Surface site —fluid associating interaction is also represented by a square-well potential with $r_c = 1.2$ and associating strength $\varepsilon_{aw} = 20$. In this study, surface is placed at $z = 0$ and active sites are placed on the top of the virtual surface molecules. The centers of virtual molecules are located at z = −0.5. We have kept the surface particle radius the same as that of the fluid molecules. In this work, site density, ρ_s, represents the number of associating surface sites per unit area. ρ_s is fixed at 1.0 unless otherwise stated.

2.2. Methodology. Grand canonical transition matrix Monte Carlo[45] simulation along with histogram reweighting[46] is employed in this work. GC-TMMC simulations are conducted in a grand-canonical ensemble at a constant chemical potential μ, volume V, and temperature T.

In transitional matrix Monte Carlo approach,[47] we record attempted transitions between microstates of different densities during moves in a collection matrix. In this work, four basic Monte Carlo (MC) moves are used, namely, displacement, insertion and deletion, and rotation moves.[48] Macrostate probability is evaluated using the detailed balance expression and collection matrix. At regular intervals, we utilize the updated macrostate probability to bias the sampling toward low probability densities using a multicanonical sampling technique.[49]

This methodology eventually leads to an efficient sampling over time for all densities of interest. Such a simulation is

conducted at a given chemical potential; hence, with the probability distribution collected at the given value of chemical potential, the histogram reweighting[46] method is used to obtain the probability distribution at other values of the chemical potential. We apply the histogram reweighting[46] technique recursively on the probability distribution by changing the chemical potential until we obtain a probability distribution, Π_N^{coex}, such that areas under the thin and thick film regions in the probability distribution plot are equal. Densities of coexisting phases are calculated from the first moment of Π_N^{coex} distribution. Details of GC-TMMC simulation techniques are given elsewhere.[45]

GC-TMMC with a finite size scaling approach can also be used to obtain the interfacial tension, also known as boundary tension,[50] between coexisting thin and thick films. The interfacial energy for a finite-size system with a substrate length, L, can be determined from the maximum likelihood in the thick film $\prod_{max}^{thick}$ and thin film regions $\prod_{max}^{thin}$ and minimum likelihood in the interface region $\prod_{min}$.

$$\beta F_L = \frac{1}{2}(\ln \Pi_{max}^{thin} + \ln \Pi_{max}^{thick}) - \ln \Pi_{min} \qquad (3)$$

The interfacial free-energy of a thin thick film on a two-dimensional surface varies with the system size according to Binder's formalism.[51]

3. SIMULATION DETAILS

Bulk simulations are carried out in a cubic cell with cell length 8 to obtain the bulk saturation chemical potential with periodicity in three dimensions. Cell length 6 is used only for lower temperature systems. Surface phase transition simulations are performed with a surface, kept at the lower XY plane of the cell. Surface dimension is same as the XY plane of the cell. The simulations, in this work, are conducted with $L_x = L_y = 9$. A repulsive wall is kept at a height larger than the substrate edge length. Different heights, $L_z = 20, 40, 80$, and 120 are used for lower temperatures to ensure that the hard wall has no affect on the properties. At lower temperatures system size effect is negligible (within $1-4\%$). However, at higher temperatures, closer to the prewetting critical temperature, substantial larger substrate area, 12×12, is used to avoid system size effect on the phase transition.

In this work, trials are performed with probability 0.1, 0.35, 0.35, 0.1, and 0.1 for displacement, addition, deletion, rotation, and bias moves, respectively. The unbonding–bonding (UB) technique[52] is used to enhance the sampling. Further, the multicanonical sampling technique is employed to force the system to sample the low probability states. Multiple cores $(8-32)$ are used following the procedure employed by earlier workers.[53] Splitting the transition matrix among different cores is particularly an attractive part of the GC-TMMC methodology, which allows sampling of all the important phase states leading to efficient calculation of phase equilibria. Boundary tension calculation is performed using finite size scaling with substrate areas 144, 256, and 400. A corresponding maximum number of particles in the simulations ranges from 500 to 3000. Four independent simulations are conducted to calculate the statistical error.

4. RESULTS AND DISCUSSIONS

We report phase diagrams in terms of excess adsorption as described by earlier workers[53]

$$N^{excess}(\mu) = \langle N(\mu) \rangle - \rho_b V \exp[\beta(\mu - \mu_b)] \qquad (4)$$
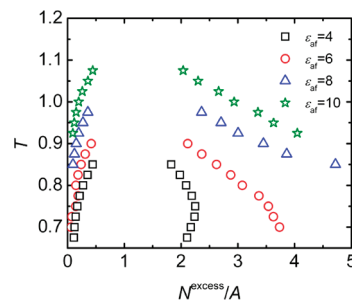

Figure 2. Surface phase coexistence curves for different associating strengths. Statistical error is smaller than the symbol size.
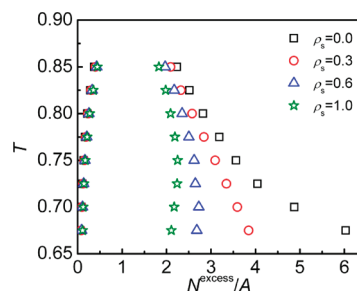

Figure 3. Surface phase coexistence curves for $\varepsilon_{af} = 4$ at different surface site densities.

where $\langle N(\mu) \rangle$ is the average number of particles in thin and thick films. ρ_b and μ_b are the density and chemical potentials of the bulk phase, respectively. In the above expression, the number of particles in the bulk phase away from the surface is corrected for any other chemical potential according to the ideal gas approximation. The error in eq 4 is found to be within 1% if the system size is also taken into consideration particularly at higher temperature as shown in our earlier work.[43] Bulk chemical potentials for the associating model are taken from our previous work.[43]

We start our discussion with Figure 2, which presents the surface phase diagram of associating fluids with various association strengths on a functional surface. The effect of increasing associating strength, in general, is to increase the density of the thick film and decrease the density of the thin film akin to that seen for associating fluids in bulk[48,54] and near a structureless surface.[43] In the case of higher associating strength fluids with $\varepsilon_{af} = 8$ and 10, thick film density increases with decreasing temperature. This indicates the divergence of the thick film at the wetting temperature, which is a characteristic behavior of prewetting transition; whereas, for associating strength, $\varepsilon_{af} = 6$, thick film density appears to have some finite value with decreasing temperature which is in contradiction to the nature of thick film seen for the prewetting transition. Further lowering the associating strength, to $\varepsilon_{af} = 4$, results in an interesting phase diagram. Density of the thicker film is seen to increase with increasing temperature up to $T = 0.75$. This behavior is in contrast to that seen for prewetting transition. However, further increase in the temperature increases the thin film density and decreases the thick film density as seen for higher associating strength fluids. To understand such phase behavior, we have extensively studied the associating fluid with $\varepsilon_{af} = 4$ at different surface site densities (ρ_s) and the results are shown in Figure 3. Figure 3 shows
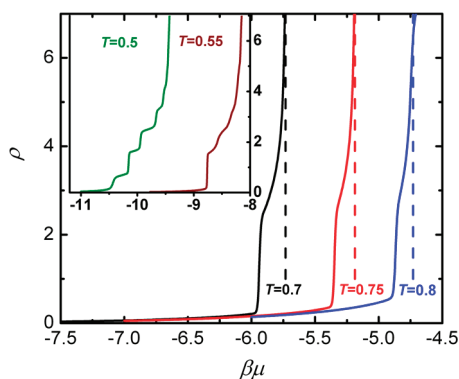
Figure 4. Adsorption isotherm for $\varepsilon_{af} = 4.0$ and $\rho_s = 1.0$ at different temperatures. The inset represents the adsorption isotherms for lower temperature range (lower than the temperatures shown in the phase diagram (Figure 3)). Dash lines represent the bulk saturation chemical potential.

divergence of the thick film density with decrease in temperature for the smooth surface ($\rho_{s,} = 0.0$), which is evidence of the prewetting transition. However, presence of sites on the surface changes the nature of the phase diagram, and thicker film no longer is seen to diverge at lower temperature. In fact, at $\rho_s = 1.0$, thick film density is observed to have a peculiar behavior of maximum density at an intermediate temperature. We resort to adsorption isotherms and density profiles to understand such anomalous behavior of low associating fluids on a functionalized surface with strong surface sites.

Figure 4 presents the adsorption isotherms for $\varepsilon_{af} = 4$ and $\rho_s = 1.0$ at different temperatures (corresponding to the temperature range shown in Figure 2). Adsorption isotherms clearly indicate first-order transition between thin and thick films. Further decreasing the temperature, $T < 0.60$, splits the first-order thin—thick transition into layering transitions, which is shown in the inset of Figure 4. At lower temperatures, $T \leq 0.55$, vapor—liquid transition is not observed implying that these temperatures could be very close to triple point or below the triple point. Similar observation is also predicted theoretically for many systems like chain molecules[29,55] and associating fluids[26] on attractive surface. This behavior is also noticed experimentally for binary liquid—solid interface.[56] We notice the rounding nature of the layering transitions. Such behavior is mainly due to the system size effect as also reported by several workers.[57−61]

Interestingly, increase in temperature, for instance from $T = 0.7$ to 0.75, slightly thickens the thick film which is contrary to the prewetting transition behavior. It is observed that functionalization of the surfaces particularly with high site density suppresses the prewetting transition. It is shown by earlier workers that layering transitions may interfere with the prewetting transition[26] in cases where the wetting temperature is below the roughening temperature. This is also evident from the surface phase diagram where with increasing temperature thick film density increases up to a certain temperature and then decreases as normally seen for a prewetting transition. The suppression (or disappearance) of a prewetting transition on a functional surface of high site density may be due to the interference of layering transitions up to a certain temperature. Layering transition, in this work, is mainly due to the surface strength caused by bonded molecules. Hence, a bonded molecule fraction for each temperature may have some information about this anomaly, which is discussed later.

While high surface site density displays a layering transition, lowering the site density separates out prewetting transition from layering transition as seen from Figure 3. As expected, a strong surface induces a layering transition at lower temperatures while a weak surface leads to a prewetting transition. To provide more insight to the interesting shift in the nature of surface transition, we move to density profiles at various surface site densities.

Figure 5 shows the density profile of two coexistence phases for $\varepsilon_{af} = 4$ at different temperatures with different surface site densities. The first peak in the density profiles of the two phases is due to the site—site interaction of fluid molecules with substrate, also referred to as the bonded region by Tripathi and Chapman.[21] In this region, molecules that are associated to substrate and fluid sites are oriented toward the surface. The number of bonded molecules increases with increase in surface site density and/or with decrease in temperature as seen from Figure 5. This region is due to the active sites and is not seen for associating fluids on smooth surfaces.[43] Figure 5a shows a typical surface density profiles on a surface-active substrate with $\rho_s = 0.3$ for different temperatures. The effect of temperature on the thick and thin films is as expected; i.e., a decrease in the temperature increases the number of density peaks. This is more prominent at a lower surface site density, $\rho_s = 0.3$. At a higher density of the active sites, $\rho_s = 1.0$, the number of layers of fluid density in the thick film is not sensitive to the change in the temperature indicative of the change in the nature of phase transition (see Figure 5b). In addition, the thick film density region shrinks with increasing surface active sites as seen from Figure 5c. Interestingly, a thin film is indifferent to the surface site densities. The density profile clearly indicates that surface sites, with appropriate site density, can suppress the growth of the thick film for the associating fluid with $\varepsilon_{af} = 4.0$. To quantify the anchoring effect of the bonding region to the subsequent layers, we have analyzed the energy profiles of thin and thick films, as shown in Figure 5d, across the z direction, for different site densities. The density profile suggests that the first two peaks are very close to each other ($z \approx 0.70$ and $z \approx 1.0$). Hence, it is expected that the energy of the bonding region should have some significant effect on subsequent layers. This is indeed the case. For example, for site density $\rho_s > 0.3$, the energy of bonding region is quite high, which is responsible for decrease in energy of subsequent layers and hence suppresses the thick film growth (such is not the case for low bonding energy region, for $\rho_s < 0.3$). On the other hand, energy of the bonding region for thin films is quite low to affect subsequent layers. Hence, thin film density is indifferent to site density which is also seen from density profiles. We have also examined the bonded region for obtaining any signature which may provide some insight to the change in the nature of the surface transition with increasing surface site density. Typical configuration snapshots of thick films for $\varepsilon_{af} = 4.0$ and their corresponding bonded molecules are shown in Figure 6. Molecules in the bonded region decrease with increase in temperature as well as decreasing surface site density. With decrease in temperature from $T = 0.75$ to $T = 0.70$, molecules in the bonded region significantly increase as can be seen in panels a and b of Figure 6 without any growth in thick film. There is a slight reorganization among molecules in the bonded region with subsequent layers which is also seen from the density profiles. Separate calculation of molecules in the bonded region reveals that there is a peculiar behavior noted for systems with higher site densities $\rho_s > 0.3$. Change in temperature from
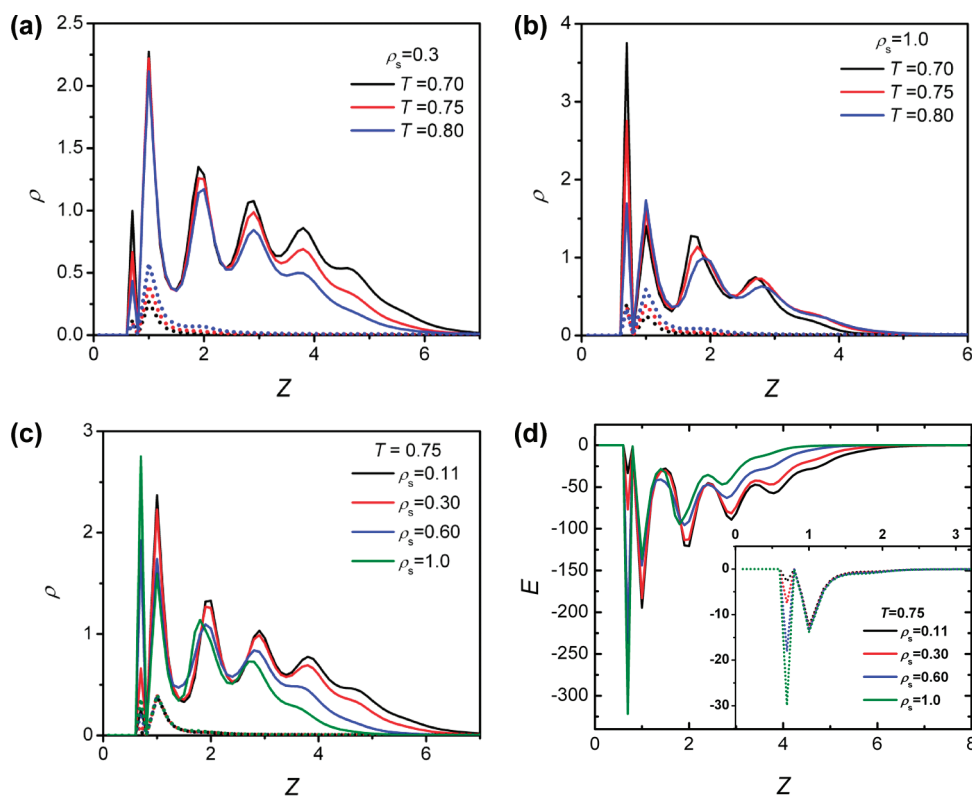
Figure 5. Local number density profile for coexistence phases for $\varepsilon_{af} = 4.0$ at (a) $\rho_s = 0.3$, (b) $\rho_s = 1.0$, and (c) $T = 0.75$. (d) Local energy profile for thin and thick films at different surface site densities. Dotted lines correspond to quasi-2D vapor phase and solid lines correspond to quasi-2D liquid phase.
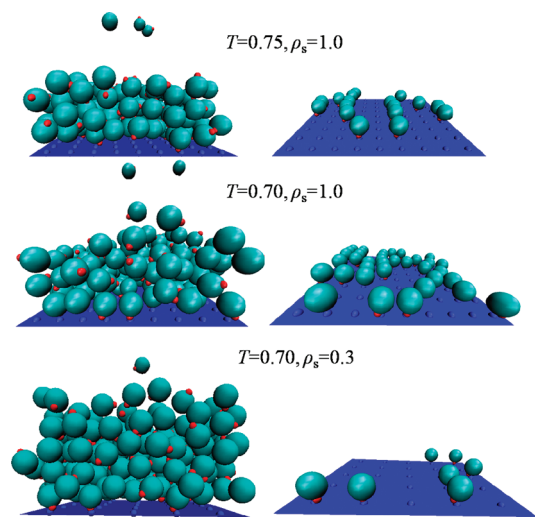

Figure 6. Configuration snapshots of thick films (left panel) and corresponding bonded region molecules (right panel) at (a, top) $T = 0.75$ and $\rho_s = 1.0$, (b, middle) $T = 0.70$ and $\rho_s = 1.0$, and (c, bottom) $T = 0.70$ and $\rho_s = 0.3$.

Figure 7. Difference of bulk saturation chemical potential and chemical potential for surface phase transition vs temperature for $\varepsilon_{af} = 4$.

interaction strength compared to the fluid—fluid interaction strength. We expect such behavior for other associating strengths also but with appropriate strength and density of the surface site.

It is argued, theoretically,[62] that in the case of prewetting transition, $\Delta\mu$ (difference between the bulk and prewetting chemical potentials) scales as $(T - T_w)^{3/2}$ for surface potential with van der Waals tail $\sim 1/z^3$. This is also observed for associating fluids on a smooth surface.[43] However, such a relation does not hold for quasi-2D vapor liquid transition;[33] on the contrary, $\Delta\mu$ was found to increase with decrease in temperature for quasi-2D vapor liquid transition of a square-well fluid on a smooth square-well surface.[33] To analyze the phase transition of

$T = 0.75$ to $T = 0.70$ increases the number of bonded molecules by more than 100% which is sufficient enough to suppress the growth of the thick film and yields maxima in the thick film density at $T = 0.75$, as seen from surface phase diagram for $\varepsilon_{af} = 4.0$ (see Figure 2). It should be noted that the crossover in the nature of surface phase transitions, what we observed in this work, depends strongly on the site density and site—fluid
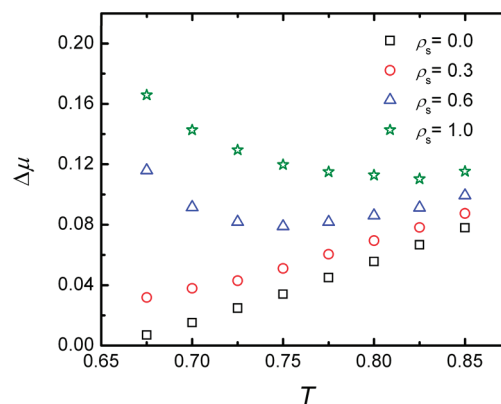
17865

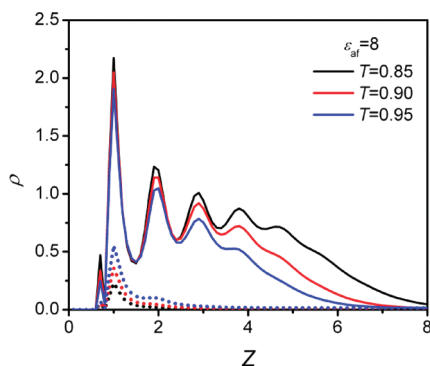dx.doi.org/10.1021/jp204025e |J. Phys. Chem. C 2011, 115, 17861–17869

Figure 8. Local number density profile for coexistence thick and thin films for $\varepsilon_{af} = 8$ at different temperatures. Dotted lines correspond to thin films and solid lines correspond to thick films.

associating fluids on functionalize surfaces, we have calculated $\Delta\mu$ for a range of temperatures for the determination of the type of the transitions. In the case of prewetting temperature, $\Delta\mu$ should approach zero (toward the bulk saturation line) with decreasing temperature. To this end, we have determined the difference between the bulk saturation and the surface phase transition coexistence chemical potentials, $\Delta\mu$, as a function of temperature for $\varepsilon_{af} = 4$, and this is shown in Figure 7. A prewetting transition is observed for $\rho_s = 0.0$ (smooth surface) and $\rho_s = 0.3$. This is also evident from Figure 5a where we noticed increase in layer densities of the thick film with decreasing temperature. However, at higher surface densities, $\Delta\mu$ decreases slightly, initially, with decrease in temperature and, subsequently, increases. This behavior suggests that thick film density no longer diverges for these cases, which can be seen from the density profile in Figure 5b. Figure 7 suggests strongly that there is a crossover from prewetting to quasi-2D vapor−liquid transition for higher surface active densities, $\rho_s > 0.3$, for associating fluid $\varepsilon_{af} = 4$. Increase in $\Delta\mu$ at lower temperatures, for $\rho_s > 0.3$ is attributed to the quasi-2D vapor−liquid transition followed by layering transition as seen clearly in Figure 4.

While crossover behavior is clearly visible for associating fluid with $\varepsilon_{af} = 4$ on an active surface, prewetting transition still is intact for a higher associating system, $\varepsilon_{af} = 8$ and 10. This is evident from the density profile where growth of the thick film is clearly visible with decrease in temperature (see Figure 8). It should be stated that the bonding region is still present for higher associating fluids but it no longer suppresses the growth of the thick film. It is quite likely that stronger (much greater than 20) strength of the surface sites may induce quasi-2D vapor−liquid transition for associating systems, $\varepsilon_{af} = 8$ and 10. Such analysis requires extensive simulations and is not in the current scope of this work.

Bonding information or monomer fraction provides significant insight to molecular arrangement. In this work, monomer fraction is determined by the fraction of total molecules, which are in the nonbonded state. It is of interest to understand the difference in bonded or nonbonded arrangement for current system to obtain a signature in the bonding information for the crossover behavior. To this end, we have calculated the monomer fraction of thin and thick films for various associating fluids on a functional surface with $\rho_s = 1.0$. The nature of the phase diagram for monomer fraction is similar to that of smooth surface[43] but with little change in magnitude of the monomer fraction values.
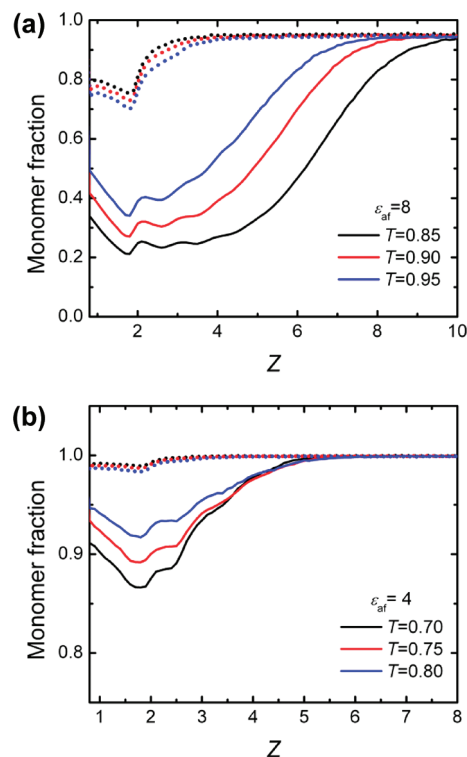

Figure 9. Coexistence monomer fraction profile for two films at different temperatures for (a) $\varepsilon_{af} = 8$ and (b) $\varepsilon_{af} = 4$. Dotted lines are for thin films and solid lines are for thick films.

Nonetheless, the overall nature of monomer fraction in thin and thick films as a function of temperature is similar for $\varepsilon_{af} = 4$ and 8 and does not provide any evidence of different types of transitions. We resort to a monomer fraction profile in the search of evidence for features of the surface phase transitions in the bonding information. Panels a and b of Figure 9 present the monomer fraction profile for $\varepsilon_{af} = 8.0$ and $\varepsilon_{af} = 4.0$, respectively. Though the nature of the curves is not different from that seen for $\varepsilon_{af} = 8.0$, the degree of bonding in thin and thick films is significantly lower for $\varepsilon_{af} = 4.0$. The noteworthy difference between $\varepsilon_{af} = 8.0$ and 4.0 cases is the extent of bonding region away from the surface. For $\varepsilon_{af} = 4.0$, a monomer fraction in the thin film is insensitive to the change in temperature. On the other hand, thicker film bonding is affected by lowering the temperature; however, bonding region do not get extended further away from the surface for $\varepsilon_{af} = 4.0$ which is in contrast to the behavior seen for thick film for $\varepsilon_{af} = 8.0$ where lowering the temperature increases the range of the bonded region. This suggests that, for associating fluids, extent of the bonding region as a function of temperature may provide a signature of prewetting transitions.

Associating molecules being anisotropic in nature are expected to have density, temperature, and surface characteristics based orientational behavior. To understand orientation behavior of particles in thin and thick films, we have used an order parameter, S, which is defined as

$$S = \left\langle \frac{3\cos^2\theta - 1}{2} \right\rangle \tag{5}$$

where θ is the angle between z axis, unit vector normal to the surface, and the associating site of the molecule. We have examined the orientational behavior of thin and thick films for
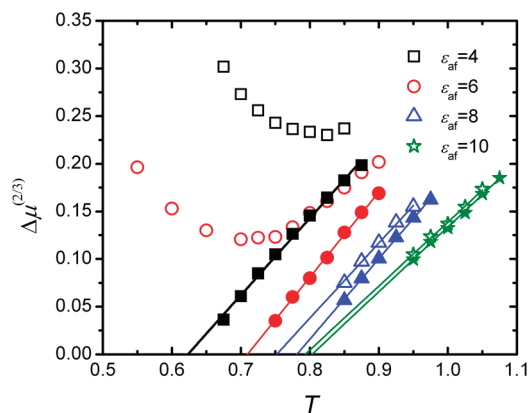
Figure 10. Difference of bulk saturation chemical potential and chemical potential for surface phase transition vs temperature for one site associating fluids. Filled and open symbols represent the data for smooth and functional surfaces, respectively.

Table 1. Wetting Temperature, T_w, and Surface Critical Temperature T_{sc},[33] for Various Association Strengths, ε_{af} on a Functional Surface with $\rho_s = 1.0$, Reduced by Bulk Critical Temperature, T_{bc}[a]

	smooth surface[43]			functional surface		
			$(T_{pwc} - T_w)/$			$(T_{sc} - T_w)/$
ε_{af}	T_w/T_{bc}	T_{pwc}/T_{bc}	T_{bc}	T_w/T_{bc}	T_{sc}/T_{bc}	T_{bc}
4	0.522	0.727	0.205		0.699	
6	0.583	0.757	0.174		0.744	
8	0.622	0.791	0.169	0.599	0.793	0.194
10	0.604	0.814	0.210	0.597	0.802	0.205

[a] T_{sc} should be read as prewetting critical temperature, T_{pwc}, for $\varepsilon_{af} = 6$ and 8. We also include T_{pwc} and T_w data for a smooth surface from our earlier work,[43] for comparison. The errors, in the critical temperatures, calculated as 1 standard deviation of the mean of four independent runs, are less than 1%.

quasi-2D and prewetting transitions (figure not shown). Interestingly, orientational behavior is found to be indifferent to the site density and the fluid molecules in the bonding region are approximately oriented normal to the surface in both the films.

Now we turn our attention to prewetting critical temperature and wetting temperature. It is well-known that prewetting transition stems from the saturation curve at the wetting temperature.[6] In this work, we have evaluated the difference between the bulk saturation chemical potential and prewetting chemical potential, $\Delta\mu$, for a series of temperatures and extrapolated it to zero to determine the wetting temperature. Prewetting critical temperature calculation, on the other hand, is calculated by extrapolating a set of boundary tensions (the tension between thin and thick films) to the temperature where boundary tension between thick and thin films vanishes. The details of boundary tension calculation are presented in the next section.

Figure 10 presents the difference of bulk saturation and prewetting chemical potential, $\Delta\mu$, as a function of temperature, in the scaling form, $\Delta\mu^{2/3}$ vs T. The prewetting behavior is clearly seen for $\varepsilon_{af} = 8$ and 10. Wetting temperature, evaluated from linear regression analysis of the data points, is seen to increase
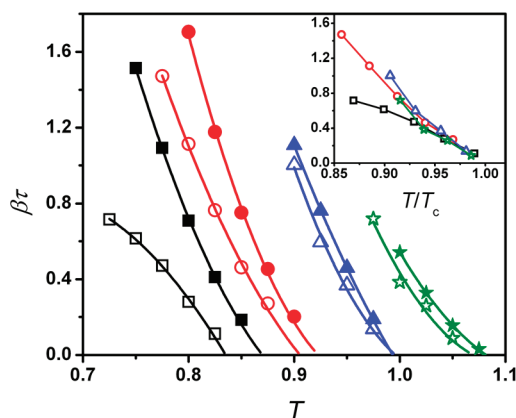

Figure 11. Infinite system size boundary tension vs temperature for various association strengths. Symbols square, circle, triangle, and star represent $\varepsilon_{af} = 4$, 6, 8, and 10, respectively. Filled and open symbols represent the data for smooth and functional surface, respectively. Curves serve as a guide to the eye.

with increasing association strength but is less compare to that seen for the smooth surface.[43] Wetting temperatures calculated, in this work, are reported in Table 1. In the case of $\varepsilon_{af} = 6$ the trend in the $\Delta\mu(T)$ behavior with decreasing temperature, started initially as per the expected behavior of prewetting transition; however, at lower temperatures there is a transition and $\Delta\mu$ instead starts increasing. This indeed is an indication of disappearance of the prewetting behavior, which entirely could not be easily detected from the set of density profiles. It is noteworthy that difference in the behavior between functional and smooth surfaces reduces with increase in the strength of the associating fluid.

In this work, boundary tension behavior is also analyzed for associating fluids on functional surfaces. The finite size scaling method of Binder is used to obtain the true boundary tension from the extrapolation of a series of finite size interfacial tension. Figure 11 presents the boundary tension of different associating fluids, as obtained from Binder's method, for a functional surface. Boundary tension decreases with increase in the temperature and approaches zero at prewetting critical temperature. Prewetting critical temperature, in this work, is calculated from second-order polynomial fit to the boundary tension values. This behavior, in general, is similar to that seen in our earlier work on associating fluid on a smooth surface.[43] Boundary tension behavior with temperature for $\varepsilon_{af} = 4.0$ surprisingly has a different curvature, which could be attributed to its quasi-2D vapor−liquid behavior. Boundary tension is found to reduce in the presence of active sites compared to that seen for a smooth surface[43] and so is true for prewetting critical temperature. The effect of active sites though is significantly less for higher associating fluids. Reduced plot suggests that boundary tension of quasi-2D transition is considerably lower than that of prewetting transition. This is in agreement with our earlier work on nonassociating fluids.[33]

■ CONCLUSIONS

We have examined the influence of associating strength on surface phase transition, monomer fraction, density and energy profiles, and boundary tension in the presence of surface sites. Crossover behavior between quasi-2D vapor liquid transition and prewetting transition is found for associating strength 4 at a

certain $\rho_s > 0.3$. We also observed quasi-2D vapor−liquid transition for the system with $\varepsilon_{af} = 6$ and with $\rho_s = 1.0$. In the case of quasi-2D vapor liquid transition, we have noticed that the growth of thick films is suppressed with decrease in temperature and finally splits in layering transitions. Layering transitions are more pronounced at high surface site density. In particular, for $\varepsilon_{af} = 4$ and $\rho_s = 1.0$ the growth of thick film even decreases with decrease in temperature, whereas for prewetting transition, the growth of thick film increases with decrease in temperature and finally wets the surface at the wetting temperature. Coexistence chemical potential for quasi-2D vapor liquid transition shifts away from the vapor liquid saturation line with decrease in temperature, while for prewetting transition, coexistence chemical potential meets bulk saturation chemical potential at the wetting temperature. Surface−fluid associating strength, 20, is considerably larger for $\varepsilon_{af} = 4$ and 6 to induce quasi-2D vapor−liquid transition. However, for stronger associating fluid, for the same functional surface, prewetting transition prevails. Monomer fraction for both quasi-2D and prewetting transitions is similar in nature. However, monomer fraction profile for $\varepsilon_{af} = 4.0$ and 8.0 does bear a signature of different types phase transition within the extent of dimerization range with lowering of the temperature. At higher associating strength wetting temperature increases with increasing associating strength but the value is comparatively lower than that seen for smooth surface; however, prewetting critical temperature seems to be insensitive to site densities which is also predicted by DFT.[26] We have also examined the boundary tension using finite size scaling for associating fluids. Boundary tension is found to reduce in the presence of active sites. This is more predominant in relatively weaker associating fluids. A reduced plot of boundary tension suggests significant lower values for quasi-2D transitions compared to that of prewetting transitions.

This work, using molecular simulation, clearly describes tuning the surface phase transition for associating fluids using active sites on the surface. The current work would be useful for the development of theoretical approaches such as DFT, which could be used to properly estimate the site densities for various associating fluids for the crossover behavior.

■ AUTHOR INFORMATION

Corresponding Author
*E-mail: jayantks@iitk.ac.in.

■ ACKNOWLEDGMENT

■ REFERENCES

(1) Jackman, R. J.; Wilbur, J. L.; Whitesides, G. M. *Science* **1995**, *269*, 664.
(2) Reisch, A.; Voegel, J. C.; Gonthier, E.; Decher, G.; Senger, B.; Schaaf, P.; Mesini, P. J. *Langmuir* **2009**, *25*, 3610.
(3) Rampi, M. A.; Whitesides, G. M. *Chem. Phys.* **2002**, *281*, 373.
(4) Wu, C.; Chen, M.; Xing, C. *Langmuir* **2010**, *26*, 15972.
(5) Sung, K. E.; Vanapalli, S. A.; Mukhija, D.; McKay, H. A.; Millunchick, J. M.; Burns, M. A.; Solomon, M. J. *J. Am. Chem. Soc.* **2008**, *130*, 1335.
(6) Cahn, J. W. *J. Chem. Phys.* **1977**, *66*, 3667.
(7) Ebner, C.; Saam, W. F. *Phys. Rev. Lett.* **1977**, *38*, 1486.
(8) Finn, J. E.; Monson, P. A. *Phys. Rev. A* **1989**, *39*, 6402.
(9) Rutledge, J. E.; Taborek, P. *Phys. Rev. Lett.* **1992**, *69*, 937.
(10) Ketola, K. S.; Moreau, T. A.; Hallock, R. B. *J. Low Temp. Phys.* **1995**, *101*, 343.
(11) Phillips, J. A.; Ross, D.; Taborek, P.; Rutledge, J. E. *Phys. Rev. B* **1998**, *58*, 3361.
(12) Cheng, E.; Mistura, G.; Lee, H. C.; Chan, M. H. W.; Cole, M. W.; Carraro, C.; Saam, W. F.; Toigo, F. *Phys. Rev. Lett.* **1993**, *70*, 1854.
(13) Kruchten, F.; Knorr, K. *Phys. Rev. Lett.* **2003**, *91*, 0855021.
(14) Zhao, X. *Phys. Rev. B* **2007**, *76*, 0414021.
(15) Kellay, H.; Bonn, D.; Meunier, J. *Phys. Rev. Lett.* **1993**, *71*, 2607.
(16) Ragil, K.; Meunier, J.; Broseta, D.; Indekeu, J. O.; Bonn, D. *Phys. Rev. Lett.* **1996**, *77*, 1532.
(17) Bahr, C. *Europhys. Lett.* **2009**, *88*, 46001.
(18) Gelb, L. D.; Gubbins, K. E.; Radhakrishnan, R.; Sliwinska-Bartkowiak, M. *Rep. Prog. Phys.* **1999**, *62*, 1573.
(19) Vega, L. F.; Muller, E. A.; Rull, L. F.; Gubbins, K. E. *Adsoroption* **1996**, *2*, 59.
(20) Vakarin, E.; Duda, Y.; Holovko, M. *J. Chem. Phys.* **1997**, *107* 5569.
(21) Tripathi, S.; Chapman, W. G. *J. Chem. Phys.* **2003**, *119*, 12611.
(22) Muller, E. A.; Vega, L. F.; Gubbins, K. E.; Rull, L. F. *Mol. Phys.* **1995**, *85*, 9.
(23) Malo, B. M.; Pizio, O.; Patrykiejew, A.; Sokolowski, S. *J. Phys: Condens. Matter* **2001**, *13*, 1361.
(24) Kovalenko, A.; Pizio, O.; Henderson, D.; Sokolowski, S. *J. Colloid Interface Sci.* **1996**, *182*, 407.
(25) Huerta, A.; Pizio, O.; Bryk, P.; Sokolowski, S. *Mol. Phys.* **2000**, *98*, 1859.
(26) Malo, B. M.; Huerta, A.; Pizio, O.; Sokołowski, S. *J. Phys. Chem. B* **2000**, *104*, 7756.
(27) Patrykiejew, A.; Salamacha, L.; Sokołowski, S.; Pizio, O. *Phys. Rev. E* **2003**, *67*, 061603.
(28) Chen, C.-C.; Dormidontova, E. E. *Macromolecules* **2006**, *39* 9528.
(29) Borowko, M.; Patrykiejew, A.; Sokolowski, S.; Staszewski, T. *Collect. Czech. Chem. Commun.* **2010**, *75*, 221.
(30) Sacquin, S.; Schoen, M.; Fuchs, A. H. *J. Chem. Phys.* **2003**, *118* 1453.
(31) Bohlen, H.; Schoen, M. *J. Chem. Phys.* **2004**, *120*, 6691.
(32) Curtarolo, S.; Stan, G.; Cole, M. W.; Bojan, M. J.; Steele, W. A. *Phys. Rev. E* **1999**, *59*, 4402.
(33) Saha, A. K.; Singh, S. P.; Singh, J. K.; Kwak, S. K. *Mol. Phys.* **2009**, *107*, 2189.
(34) Singh, J. K.; Sarma, G.; Kwak, S. K. *J. Chem. Phys.* **2008**, *128* 044708.
(35) Rull, L. F.; Romero-Enrique, J. M.; Muller, E. A. *J. Phys. Chem. C* **2007**, *111*, 15998.
(36) Wyatt, A. F. G.; Klier, J. *Phys. Rev. Lett.* **2000**, *85*, 2769.
(37) Reinelt, D.; Iov, V.; Leiderer, P.; Klier, J. *J. Phys: Condens. Matter* **2005**, *17*, 403.
(38) Klier, J.; Leiderer, P.; Reinelt, D.; Wyatt, A. F. G. *Phys. Rev. B* **2005**, *72*, 245410.
(39) Rolley, E.; Guthmann, C.; Pettersen, M. S. *Phys. Rev. Lett.* **2009**, *103*, 016101.
(40) Taborek, P. *J. Low Temp. Phys.* **2009**, *157*, 101.
(41) Brovchenko, I.; Geiger, A.; Oleinikova, A. *J. Chem. Phys.* **2004**, *120*, 1958.
(42) Brovchenko, I.; Oleinikova, A. *J. Phys. Chem. C* **2007**, *111*, 15716.
(43) Khan, S; Singh, J. K. *J. Chem. Phys.* **2010**, *132*, 144501.
(44) Chapman, W. G. *J. Chem. Phys.* **1990**, *93*, 4299.
(45) Errington, J. R. *Phys. Rev. E* **2003**, *67*, 012102.
(46) Ferrenberg, A. M.; Swendsen, R. H. *Phys. Rev. Lett.* **1988**, *61* 2635.
(47) Fitzgerald, M.; Picard, R. R.; Silver, R. N. *J. Stat. Phys.* **2000**, *98*, 321.
(48) Singh, J. K.; Kofke, D. A. *J. Chem. Phys.* **2004**, 121.
(49) Berg, B. A.; Neuhaus, T. *Phys. Rev. Lett.* **1992**, *68*, 9.

(50) Errington, J. R.; Wilbert, D. W. *Phys. Rev. Lett.* **2005**, *95*, 226107.

(51) Binder, K. *Phys. Rev. A* **1982**, *25*, 1699.

(52) Wierzchowski, S.; Kofke, D. A. *J. Chem. Phys.* **2001**, *114*, 8752.

(53) Errington, J. R. *Langmuir* **2004**, *20*, 3798.

(54) Singh, J. K.; Kofke, D. *Mol. Simul.* **2004**, *30*, 343.

(55) Bryk, P.; Bucior, K.; Sokołowski, S.; Zukocinski, G. *J. Phys. Chem. B* **2005**, *109*, 2977.

(56) Hamraoui, A.; Privat, M. *J. Chem. Phys.* **1997**, *107*, 6936.

(57) Gatica, S. M.; Bojan, M. J.; Stan, G.; Cole, M. W. *J. Chem. Phys.* **2001**, *114*, 3765.

(58) Thommes, M.; Findenegg, G. H. *Langmuir* **1994**, *10*, 4270.

(59) Detcheverry, F.; Kierlik, E.; Rosinberg, M. L.; Tarjus, G. *Phys. Rev. E* **2003**, *68*, 061504.

(60) Gac, W.; Patrykiejew, A.; Sokołowski, S. *Thin Solid Film* **1997**, *298*, 22.

(61) Bojan, M. J.; Steele, W. A. *Mol. Phys.* **1998**, *95*, 431.

(62) Ancilotto, F.; Toigo, F. *Phys. Rev. B* **1999**, *60*, 9019.

17869

dx.doi.org/10.1021/jp204025e |*J. Phys. Chem. C* 2011, 115, 17861–17869